MEXICO CITY SOIL BEHAVIOR AT DIFFERENT STRAINS: OBSERVATIONS AND PHYSICAL INTERPRETATION

By J. A. Díaz-Rodríguez[1] and J. C. Santamarina,[2] Members, ASCE

ABSTRACT: The unique mechanical properties of Mexico City soils plot as extreme values on most geotechnical engineering charts. The purpose of this study is to analyze salient properties and to propose conceptual models to explain them. In particular, mechanical parameters synthesized from published laboratory data are systematically organized in terms of strain level. Three strain regions are identified. The threshold strains at the boundaries between these strain regions are examined in terms of microscale processes that participate at different strains.

INTRODUCTION

Mexico City is one of the oldest metropolises in the Western Hemisphere, occupying an ancient plain (once a lake) surrounded by mountains and inhabited by at least 16 million people spread over 1,479 sq. km. The region has high seismicity. Intense ground shaking during the September 19, 1985, Mexico earthquake (Ms surface wave magnitude 8.1 and intensity IX in parts of the city) caused many building foundations to undergo excessive settlement and tilting, resulting in either collapse or substantial damage of superstructures. More than 20,000 lives were lost, and damages were estimated at $5 billion. There is a strong correlation between the spatial distribution of damage associated with this and previous events and the location of lacustrian deposits. Hence, the role of these deposits in the performance of superstructures is undisputed.

The strain-dependent shear modulus and damping ratio play an important role in estimating the response of structures to earthquake loads. Yet there is considerable uncertainty in choosing the correct values. The strain level in a soil and other particulate materials determines the type of microscale processes activated. Therefore, soil behavior and parameters may vary significantly with the level of strain, as Fig. 1 summarizes. The purpose of this study is to systematically organize and reassess experimental studies on the behavior of Mexico City soils previously conducted by Díaz-Rodríguez and coworkers. In this case, the response is reinterpreted in terms of strain levels, and conceptual particle-level models are proposed to explain observations. Experimental data are compared against trends obtained with other soils. This study starts with a review of salient index properties for Mexico City soils.

GENERAL PROPERTIES

The sediments from Mexico City are complex mixtures of crystalline minerals and amorphous material that challenge a simple nomenclature; they are heterogeneous volcanic and lacustrine sediments with microfossils (diatoms and ostracods) and organic matter. Fig. 2 shows a selection of scanning electron microscope (SEM) photomicrographs indicative of the complexity and variety. The minerals in the clay fraction include 14 Å montmorillonite, illite, and cristobalite; in some specimens, it is possible to identify regularly interstratified chlorite-smectite, resembling tosudite (physical, chemical, and mineralogical properties are described in Díaz-Rodríguez et al. 1998). This unique sediment has been studied by various researchers. Salient references include Foreman (1955), Marsal and Mazari (1959), Lo (1962), Zeevaert (1972), Mesri et al. (1975), Peralta y Fabi (1989), and Díaz-Rodríguez et al. (1998).

The grain size distribution of Mexico City sediments corresponds to silty clays or clayey silts. The water content and void ratio are typically very high ($w \approx 220-420\%$; $e \approx 5-10$). This high water content has remained, even though sediments have been subsequently buried by many layers of soil. The retention of an open fabric is indicative of slow sedimentation rates combined with a rapid development of bonds.

The very high void ratio in Mexico City soils raises the question regarding the maximum void ratio a soil may have. In the case of monosized spherical particles, the minimum coordination number required to satisfy force equilibrium in a stable regular configuration is 6 (no friction). This corresponds to the simple cubic packing arrangement, where the void ratio $e = 0.91$. In flocculated platy particles, the simple cubic configuration corresponds to a card castle structure [SEM picture, Fig. 2(b)]. Following simple algebraic manipulations, the void ratio in this case becomes

$$e_{\text{high}} = \frac{\alpha - 1}{2} \tag{1}$$

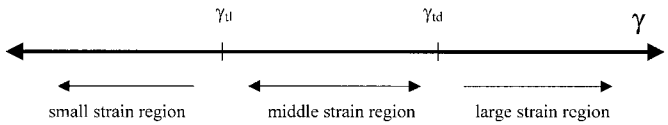

	Small Strain Region	*Large Strain Region*
Deformation mechanism	Contact deformation (constant fabric)	Fabric changes (rolling, slippage)
Stiffness	Maximum	Decreases (hyperbolic type)
Energy Losses	Very low. Viscous, thermo-elastic, (frictional: difficult to justify)	Large Frictional loss is important
Poisson's Ratio (drained)	0 - < 0.1	0.2-0.4
Volume Changes (drained loading)	Minimal	Potentially large (contraction or dilation)
Pore pressure generation (undrained loading)	Minimal	Potentially large (positive or negative)
Diagenetic effects (aging, cementation, thixotropy)	Potentially high effect	Small in drained shear. Potentially significant in undrained shear
Fabric	Constant	Changes towards critical state (eccentric particles gradually align)
Potentially opposite micro-to-macro effects. Example:	Angularity decreases small-strain stiffness (low contact stiffness)	Angularity increases large-strain stiffness (high interlocking)

FIG. 1. Strain Regions, Threshold Strains, Microscale Phenomena, and Macroscale Response. Boundaries between Different Strain Regions Correspond to Elastic Threshold Strain γ_{td} (after Santamarina et al. 2001)

[1]Prof., Dept. of Civ. Engrg., Nat. Univ. of Mexico, Apartado Postal 70-165, Mexico City 04510, Mexico. E-mail: jadrdiaz@servidor.unam.mx

[2]Prof., Dept. of Civ. and Envir. Engrg., Georgia Inst. of Technol., Atlanta, GA 30332. E-mail: carlos@ce.gatech.edu

Note. Discussion open until February 1, 2002. To extend the closing date one month, a written request must be filed with the ASCE Manager of Journals. The manuscript for this paper was submitted for review and possible publication on November 8, 1999; revised April 17, 2001. This paper is part of the ***Journal of Geotechnical and Geoenvironmental Engineering***, Vol. 127, No. 9, September, 2001. ©ASCE, ISSN 1090-0241/01/0009-0783–0789/$8.00 + $.50 per page. Paper No. 22152.

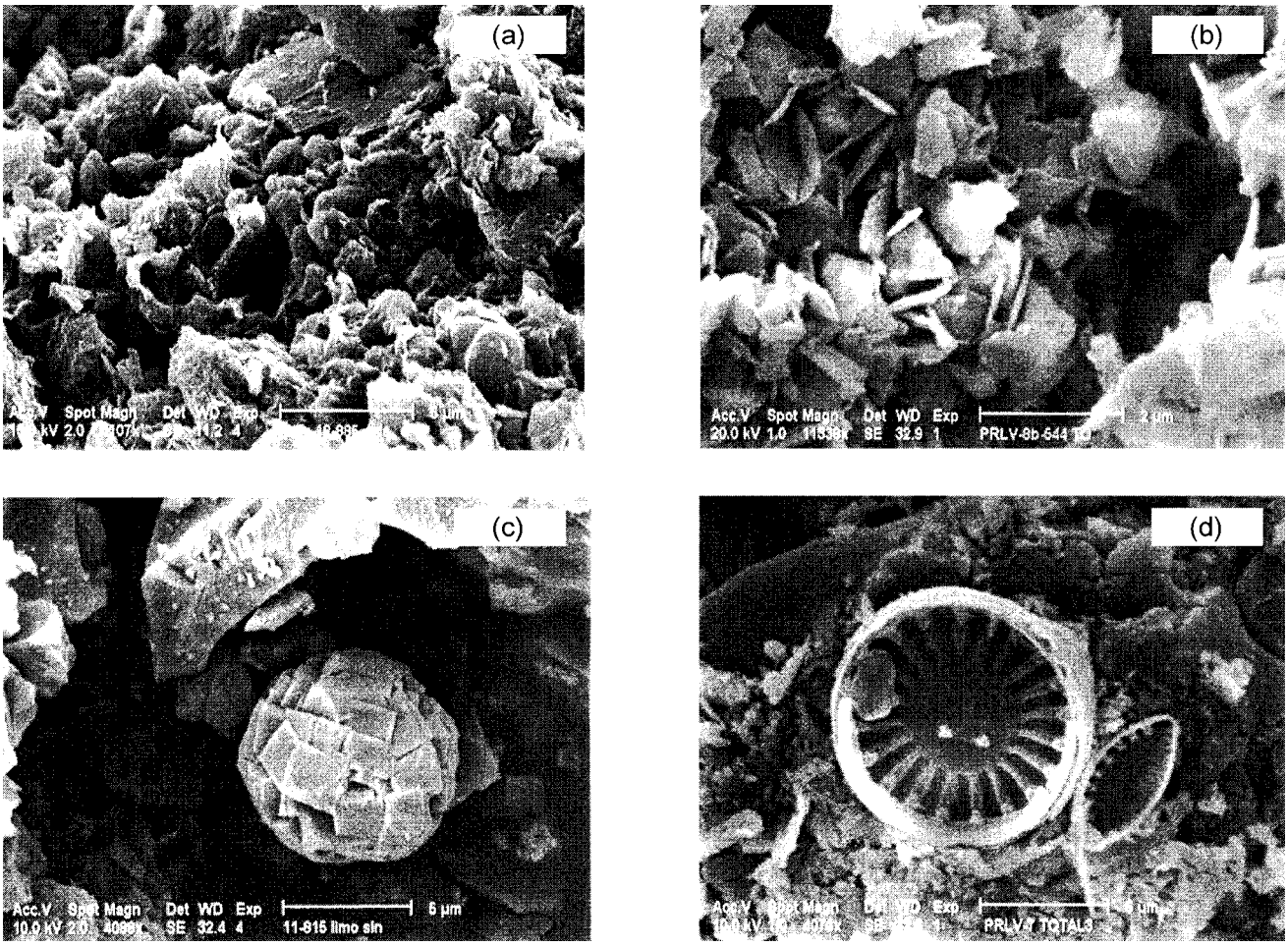

FIG. 2. Scanning Electron Photomicrographs of Specimens from Parque Ramón López Velarde: (a) Randomly Oriented Particle Domains, Including Large Voids; (b) Edge-to-Edge and Edge-to-Face Flocculated Clay Minerals; (C) Pyrite Framboid; (d) Diatom Frustules

where α = slenderness of particles defined as the length L over the thickness t; thus $\alpha = L/t$ [Fig. 3(a)]. This is not an attempt to identify the maximum void ratio, but a realizable large void ratio, albeit in a highly idealized configuration. Therefore, the maximum void ratio within aggregations formed by platy particles is linked to particle slenderness. The slenderness of kaolin varies between $\alpha = 5$ and $\alpha = 10$, suggesting possible void ratios as high as 4.5; this is confirmed by shear wave transmission in very soft kaolinite slurries (Santamarina et al. 2001). In this context, shear wave transmission is used to measure the transition from a slurry to a granular skeleton that can transmit shear. The slenderness of montmorillonite may reach $\alpha = 100$; therefore, flocculation could render void ratios as high as 50. Therefore, this analysis suggests that the high void ratio of Mexico City soils is related to the existence of aggregations formed by slender mineral plates. Other contributing factors to the high porosity of these soils is the presence of diatoms with high internal porosity [Fig. 2(d)] and the development of multiple internal scales in the soil mass, including aggregations, domains, and chains, as observed in SEM studies (Fig. 2). Intermediate scales are documented in Pusch (1970), Barden (1973), and Bennett and Hulbert (1986).

Plasticity is associated with the clay fraction in a soil. In the case of Mexico City (MC) soils, Atterberg limits are very high: liquid limit (LL) is between 110 and 458, plastic limit (PL) between 37 and 116, and corresponding plasticity index (PI) between 73 and 342. The liquid limit is the water content associated with a remolded soil at a certain undrained shear strength that varies between $S_u = 2.4$ kPa for soils with a liquid limit $LL = 30\%$ and a strength of $S_u = 1.3$ kPa for a soil with $LL = 200\%$ (Wood 1990). This strength is attained at an average interparticle distance d, reflecting the balance between interparticle contact forces, that is, skeletal contact forces and electrical forces. The water content corresponding to a particle surrounded by an average layer of water with thickness $d/2$ is [Fig. 3(b)]

$$w \approx d \cdot S_s \cdot \frac{\gamma_w}{g} \text{ (for } L >> t) \tag{2}$$

where S_s = specific surface of particles (surface area divided by mass); $\gamma_w = 9.8$ kN/m^3 is the unit weight of water; and $g = 9.8$ m/s^2 is gravity. Therefore, the liquid limit is expected to increase with the specific surface. For example, values for kaolinite are $S_s = 5-15$ m^2/g and $LL = 40-60$, and for montmorillonite, $S_s = 400-800$ and $LL = 300-700$ (Muhunthan 1991; Mitchell 1993). Farrar and Coleman (1967) obtained an empirical relation for British clays: $LL = 19 + 0.56S_s$ (for $28 < LL < 121$).

The specific surface of MC soils was determined in dry conditions by gas absorption, and in wet conditions using the methylene blue technique. The specific surface measured for the entire soil with the N_2-adsorption is $S_s = 39.8$ m^2/g, while the methylene blue technique rendered $S_s = 187$ m^2/g. The following important observations can be made: (1) The difference between specific surface values determined in dry and wet conditions confirms the presence of swelling minerals; (2) because the specific surface is determined by the fine fraction, which is about 30% of the entire soil, the specific surface estimated for the fines is 540 m^2/g—this value is in the range for swelling minerals; and (3) the high liquid limit of MC sediments reflects the high specific surface of the soil's fine fraction.

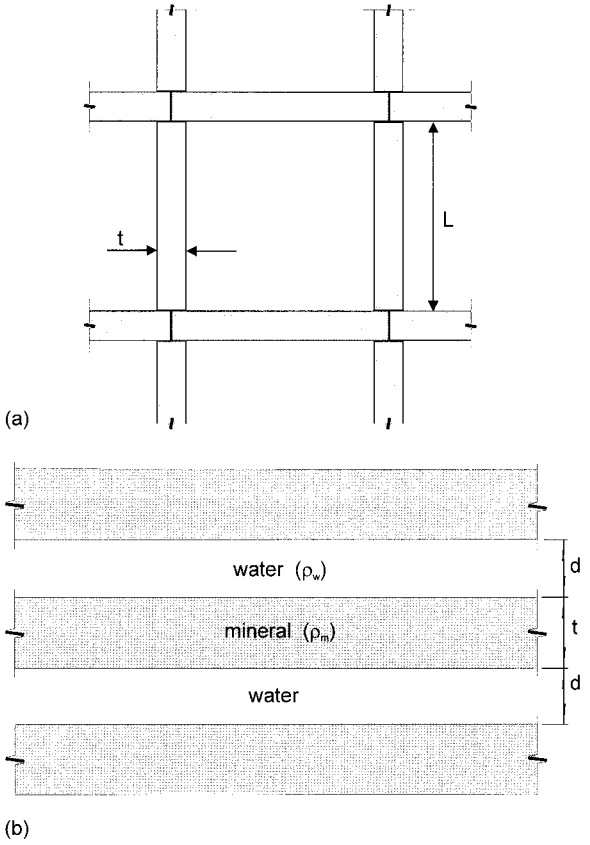

FIG. 3. Assumptions for Particle Level Analyses: (a) Realizable High Void Ratio within Aggregations—Pseudo Card Castle Arrangement of Platy Particles; (b) Average Interparticle Distance and Moisture Content in Soils Made of Platy Particles

Diagenesis has led to apparent preconsolidation (thixotropic response and mechanisms are reviewed in Díaz-Rodríguez and Santamarina 1999). According to Zeevaert (1991), the average shift between the apparent yielding pressure σ'_y and the current vertical effective stress σ'_{vo} is $(\sigma'_y - \sigma'_{vo}) = 60$ kPa. Thus, typical overconsolidation ratio (OCR) values relevant to engineering design vary between 1.1 and 1.67 (Zeevaert 1972). Data gathered by Díaz-Rodríguez and coworkers show that the apparent preconsolidation in MC soils varies with depth and with mineralogy. Published data for other clays show that the effect of aging on preconsolidation increases with the plasticity of the sediment; for example, Bjerrum (1972) shows equivalent OCR values as high as ~1.9 for a clay with PI = 100.

STRAIN REGIMES AND THRESHOLDS

Three strain regimes can be identified from the experimental data obtained with Mexico City soils (Fig. 1). In the small-strain region, the response of MC sediments is essentially linear-elastic, and no changes in microstructure occur. In the middle-strain region, the soil behavior begins displaying nonlinear behavior; however, there is minor strength degradation due to cyclic loading. The large-strain region is characterized by soil fabric destructuration leading to failure (in this context, fabric relates to the physical arrangement of particles in space).

Linear Threshold Shear Strain γ_{tl}

This threshold separates the small- from the middle-strain regime. The linear threshold strain for MC sediments is extracted from modulus degradation curves obtained with resonant column tests at a value of $G/G_0 = 0.99$. Multiple data sets point to a value that ranges around $\gamma_{tl} = 3 \times 10^{-4}$ (Díaz-Rodríguez 1992).

Degradation Threshold Strain γ_{td}

The boundary between the middle- and the high-strain regions can be defined using the following different approaches based on pore pressure generation, stiffness degradation, and strength degradation.

Vucetic (1994) selected the degradation threshold strain as when the pore pressure begins to accumulate and called it the ''volumetric threshold strain.'' Using this criterion, cyclic triaxial data for Mexico City soils presented in Fig. 4 suggest a degradation threshold strain γ_{td} = 6-to-8 $\times 10^{-3}$. For comparison, the figure also presents average trends for sands (Dobry 1989) and for kaolinite (Ohara and Matsuda 1988); PI = 25. In general, γ_{td} and γ_{tl} are about 1.5 log cycles apart; thus, $\gamma_{td}/\gamma_{tl} \approx 32$ (Vucetic 1994).

Kokusho et al. (1982) looked at the degradation in stiffness as a function of the amplitude of the cyclic shear strain. The value of γ_{td} obtained from pore pressure generation relates to a modulus reduction between 0.6 and 0.85 (Ishihara 1996). Following this approach, the volumetric threshold strain for MC sediments is γ_{td} = 4 to 8 $\times 10^{-3}$.

An alternative approach to determining the degradation

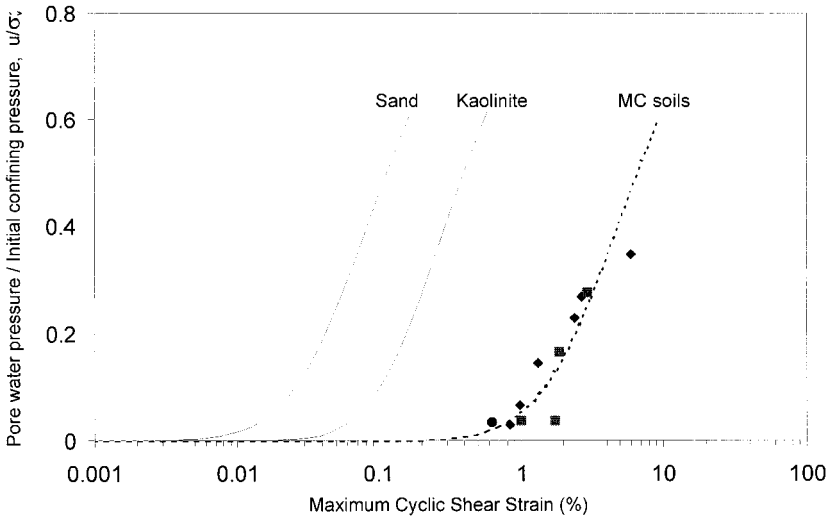

FIG. 4. Degradation Threshold Strain by Pore Pressure Accumulation. Cyclic Triaxial Test Data Gathered for Isotropically Confined Mexico City Specimens after 50 Cycles, Presented for Three Different Stress Histories: ■ $\sigma'_y/\sigma'_0 = 2.2$; ◆ $\sigma'_y/\sigma'_0 = 1.3$; and ● $\sigma'_y/\sigma'_0 = 0.8$

threshold strain is based on the degradation in strength due to cyclic loading. Díaz-Rodríguez (1989a) showed that the degradation in strength develops when the cyclic stress ratio R reaches a critical value. The methodology involves the application of initial anisotropic confinement, followed by 100 loading cycles and concluding with monotonic loading to failure, as summarized in Fig. 5(a). A typical dataset and its interpretation are shown in Fig. 5(b). Similar datasets gathered by Díaz-Rodríguez and coworkers are reevaluated in terms of cyclic strain, as shown in Fig. 6 (the strain level that is plotted is the peak strain during cyclic loading). The degradation threshold strain γ_{td} is selected at the strain level that separates the region without strength loss from the region with strength loss. In this case, the degradation threshold strain is $\gamma_{td} \approx 3 \times 10^{-2}$. The higher strain value obtained with this criterion reflects the decisive destructuring of the specimen required to attain strength loss.

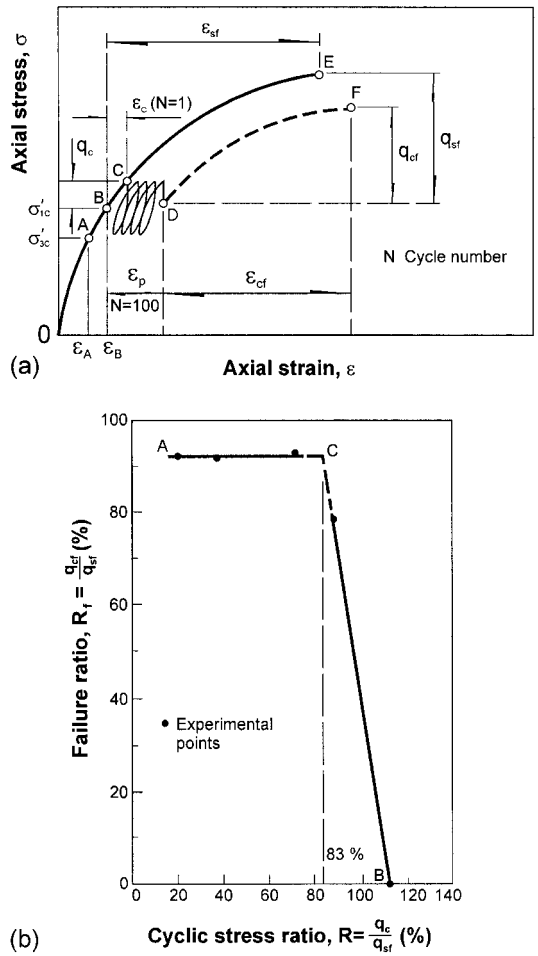

FIG. 5. Cyclic Loading and Residual Undrained Shear Strength. Degradation Threshold Strain Determined from Anisotropically Loaded Specimens. Experimental Data for $R = 0.8$ (Díaz-Rodríguez 1989a)

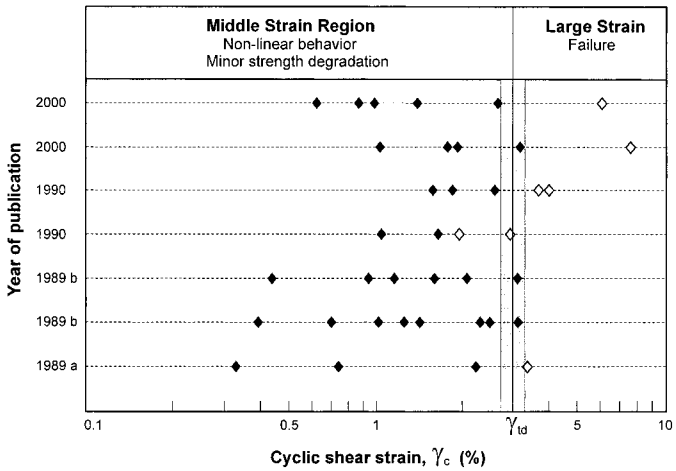

FIG. 6. Degradation Threshold Strain γ_{td}. Filled Symbols ◆ Indicate Specimens That Did Not Display Reduction in Strength after 100 Cycles; Empty Symbols ◇ Correspond to Specimens That Suffer Significant Strength Loss (Fig. 5). (Years in Left Margin Correspond to When Data Were Published by Díaz-Rodríguez and coworkers)

Microscale Interpretation

Particle-level phenomena activated in the different strain regions depend on relative displacements δ between contiguous soil particles. An order of magnitude estimation of this relative displacement is $\delta = \gamma \cdot D$, where γ is the average shear strain and D is the average particle size (for simplicity, this analysis does not address the role of the intermediate scales of domains, aggregations, and chains). This relative displacement tends to localize at interparticle contacts, and it is responsible for the breakage of interparticle bonds (including changes in repulsion and attraction forces), slippage, and the tendency toward volume change that causes pore pressure.

Presuming an average particle size for MC sediments of less than a micron, $D < 1$ μm, the threshold strain for elastic behavior, $\gamma_{tl} = 3 \times 10^{-4}$, corresponds to a relative displacement between particles $\delta \approx 3$ Å, which approaches the atomic scale. Therefore, strains lower than the elastic threshold $\gamma < \gamma_{tl}$ preserve bonds. On the other hand, an intermediate degradation threshold of $\gamma_{td} = 1 \times 10^{-2}$, which corresponds to a relative displacement between particles $\delta \approx 100$ Å, is an upper bound for long-range interparticle forces. This observation provides fundamental support to the experimental observation reported by Vucetic and Dobry (1991) whereby the volumetric threshold strain increases with the PI.

SMALL-STRAIN BEHAVIOR

The variation of stiffness and damping in the small-strain region depends on the state of stress and on the physicochemical characteristics of the soil under consideration. Díaz-Rodríguez and López-Flores (1999) ran a series of resonant column tests to assess the small-strain stiffness of MC sediments. The isotropic confinement was varied from very low effective stresses ($\sigma'_0 < \sigma'_y$) to effective stresses in excess of the yield stress ($\sigma'_0 > \sigma'_y$) when destructuration of the initial fabric is expected. Relevant observations follow. (Small-strain data are not available for anisotropically confined specimens. The potential effects of anisotropic loading on small-strain parameters are addressed in Santamarina and Cascante 1996.)

Small-Strain Stiffness

Fig. 7(a) presents the variation in stiffness G_{max} for a typical test sequence. The data are fitted with the customary power relation, $G_{max} = \chi \sigma'^{\beta}_0$ where χ and β are regression constants. Two regions are identified. Below the yield stress, in the structured region ($\sigma'_0 < \sigma'_y$), the variation in stiffness and the value of exponent β are very low. However, the exponent reaches high values above the yield stress (Fam and Santamarina 1997). Data for specimens gathered from different parks in the city are Ramon Lopez Velarde Park (LL = 304): $\sigma'_0 < \sigma'_y$, $\beta = 0.21$; $\sigma'_0 > \sigma'_y$, $\beta = 1.10$; Alameda Central Park (LL = 337): $\sigma'_0 < \sigma'_y$, $\beta = 0.27$; $\sigma'_0 > \sigma'_y$, $\beta = 0.73$.

As a reference, the exponent for various materials follows: Spherical particles with Herzian contact $\beta = 1/3$; rough particles with conical contracts $\beta = 1/2$; uncemented loose sands $\beta \approx 0.5$; uncemented dense sands $\beta \approx 0.4$; lightly cemented

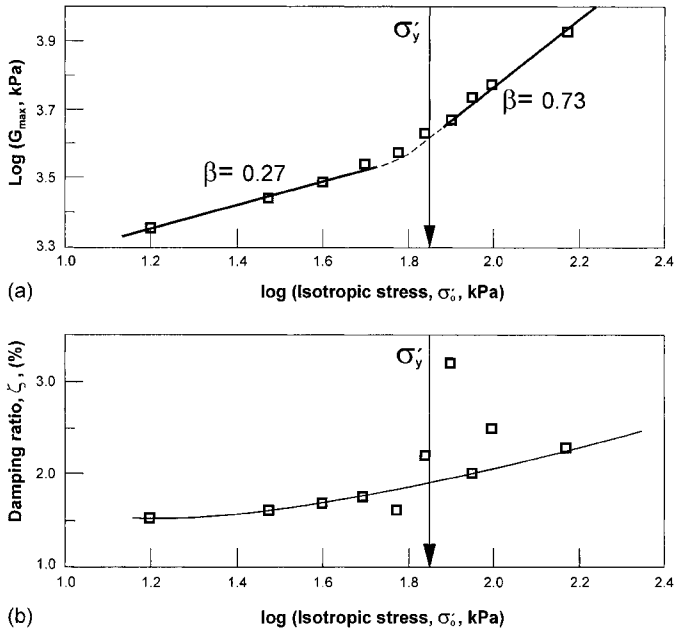

FIG. 7. Low-Strain Stiffness and Damping—Alameda Central Park (Depth = 17.4 m): Isotropic Confinement Extends from Below to Above Yield Stress of Soil. (Resonant Column Data: Shear Strain $\gamma \approx 1.2 \times 10^{-4}$; Resonant Frequency 6–10 Hz). Arrow Indicates Yield Stress σ'_y Corresponding to Specimen

sands $\beta \approx 0.1$; NC kaolinite $\beta \approx 0.6$; OC kaolinite $\beta \approx 0.3$; and NC bentonite $\beta \approx 0.85$. These data show that (1) β is higher in fine soils where double layer effects are more important; (2) β is higher for looser soils where interparticle coordination increases more readily; and (3) β is low in soils that have been subjected to diagenesis, cementation, and overconsolidation (Cascante and Santamarina 1996; Santamarina and Aloufi 1999). The first two observations explain the high exponent observed for MC sediments in the destructured zone where $\sigma'_0 > \sigma'_y$. The third observation explains the very low exponent in the structured zone where $\sigma'_0 < \sigma'_y$.

Small-Strain Attenuation

The damping ratio ζ was determined for different specimens under various conditions. Fig. 7(b) presents the data for the specimen extracted from Alameda Central Park (all specimens show similar trends). Two observations can be made: first, damping increases with confinement, and second, damping increases near the yield stress as a consequence of destructuring. The first observation indicates the overwhelming effects of viscous losses (as confinement increases, the resonant frequency increases) over frictional losses (as confinement increases, frictional losses decrease). The resonant frequency in these studies varied between 6 and 10 Hz.

Other Related Observations

In general, shear wave velocity measured in situ with crosshole tests varies little with depth ($V_s \approx 80$ m/s). In terms of shear modulus G, the back-calculated exponent $\beta = 0.22$. This low value of β suggests in situ conditions whereby $\sigma'_0 < \sigma'_y$. Furthermore, these results confirm that bonding and in situ stiffness developed before the soil experienced the applied effective stress, as discussed earlier.

An additional feature of the response at small cyclic strains is the sudden drop in stiffness and the increase in attenuation observed immediately upon load change. This has been observed in other soils (Fam et al. 1998); hypotheses are discussed in Fam and Santamarina (1997).

MIDDLE-STRAIN BEHAVIOR

Fig. 8 shows the variation in stiffness and damping with cyclic strain, when the strain level exceeds the elastic threshold, $\gamma > \gamma_{tl}$. The data correspond to the first cycle in a cyclic triaxial test (for consistency, results are plotted in terms of shear parameters). The asymptotic low-strain values are shown. Similar data are obtained for three different specimens; stiffness decreases and attenuation increases significantly in this strain region (the frequency is 0.5 Hz).

The degradation in stiffness with the number of cycles decreases with increasing plasticity and with overconsolidation (Ishihara 1996). This is clearly observed in the high-plasticity MC sediments, where diagenetic effects have caused apparent overconsolidation. A typical data set is presented in Fig. 9; while the amplitude of the applied cyclic stress is high

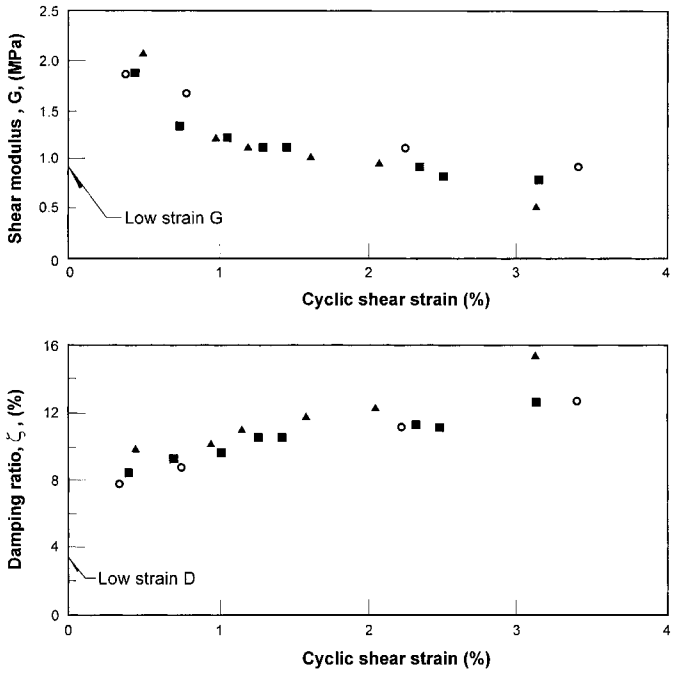

FIG. 8. Middle-Strain Region: Shear Stiffness and Damping. Experimental Data Gathered in Cyclic Triaxial. Equivalent Parameters in Shear Computed as $G = E/3$ and $\gamma = 1.5\ \varepsilon$ (Both Relations Presume $\nu = 0.5$). Circles: Anisotropic Confinement, OCR = 1. Squares: Isotropic Confinement, OCR = 1. Triangles: Isotropic Confinement, OCR = 2. Data Extracted from Díaz-Rodríguez (1989b)

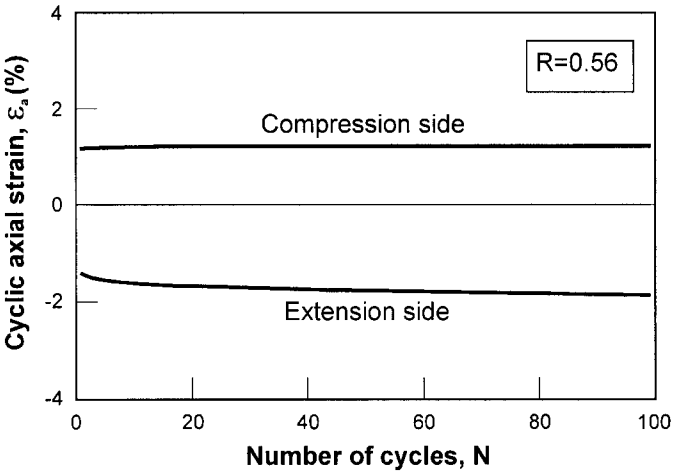

FIG. 9. Middle-Strain Region: Development for Cyclic Axial Strain during CU Cyclic Loading. Amplitude of Cyclic Stress with Respect to Undrained Shear Strength Is $R = 0.56$. Stress Controlled Test (Díaz-Rodríguez et al. 2000)

$(0.56 \cdot S_u)$, the cyclic strain remains almost constant with the number of cycles.

LARGE-STRAIN BEHAVIOR

Limited data are available to systematically extract effective stress parameters and related creep effects. Published consolidated-undrained (CU) tests with measurement of pore pressure suggest friction angles that exceed 43–46° (Marsal and Salazar-Resines 1960; Lo 1962; Mesri et al. 1975; Díaz-Rodríguez et al. 1992). The extrapolation of trends published by Kenney (1959) and Bjerrum and Simons (1960) to $PI \approx 300$, indicates friction angles as low $\phi = 5–15°$. This unexpected behavior requires careful reassessment. The presence of high intraporosity and high-roughness diatoms is one of several possible coexisting mechanisms; further investigation is in progress.

The review of strength data in terms of undrained strength c_u renders equally distinct results. Data are plotted in Fig. 10 in terms of c_u/σ_0' for different σ_y'/σ_0' ratios. The shaded region delimited by the two dotted lines corresponds to data published in Ladd and Foott (1974) for clays with plasticity ranging between $PI = 12$ and $PI = 75$. Mexico City soil data plot distinctly above the other soils and can be approximated as (Wood 1990)

$$\left(\frac{c_u}{\sigma_0'}\right)_{OC} = \left(\frac{c_u}{\sigma_0'}\right)_{NC} \text{OCR}^{\beta} = 0.85 \cdot \text{OCR}^{0.75} \tag{3}$$

The inferred normalized undrained strength for normally consolidated (NC) MC soil specimens is $(c_u/\sigma_0')_{NC} = 0.85$; however, the normalized NC strength for clays with plasticity $PI < 100$ is in the range of $(c_u/\sigma_0')_{NC} = 0.18$ to 0.4. In general, higher $(c_u/\sigma_0')_{NC}$ values should be expected for soils with higher plasticity and aging effects (Bjerrum and Simons 1960; Bjerrum 1972). The exponent $\beta = 0.75$ is similar to the value for other clays.

Destructuration by loading significantly above the yielding pressure σ_y' renders a low normalized undrained strength when thixotropic recovery is not allowed (Díaz-Rodríguez and Santamarina 1999). The data for two specimens denoted as filled circles in Fig. 10 were obtained by consolidating them to $\sigma_0' = 48.5$ kPa, while their yield pressure is $\sigma_y' = 32$ kPa. The normalized NC shear strength is $(c_u/\sigma_0')_{NC} \approx 0.65$. The normalized undrained strength is stress-path dependent in natural soils, which inherently involve some degree of anisotropy in fabric and interparticle bonds. Typically, values obtained in simple shear are lower than those determined in triaxial compression (data in Terzaghi et al. 1996). Limited data for MC soils suggest normalized shear strength from simple shear (SS) about $(c_u^{(SS)}/\sigma_0')_{NC} \approx 0.4$.

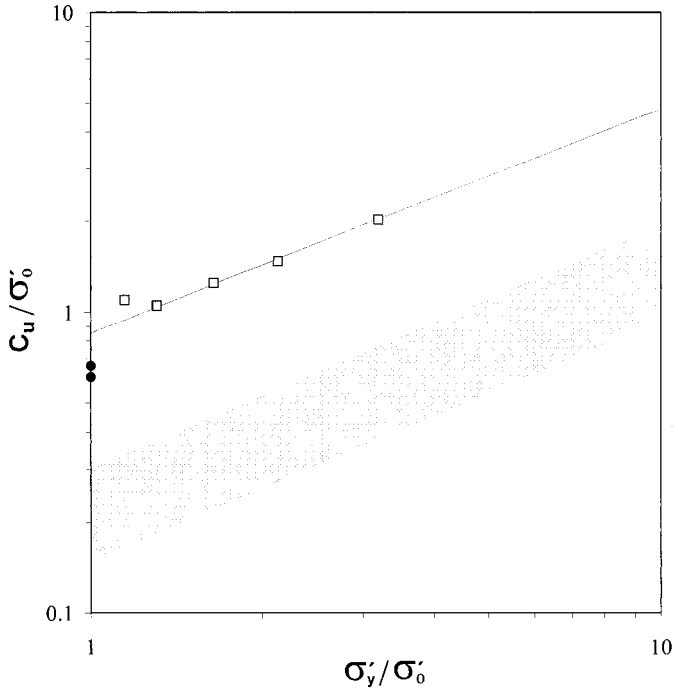

FIG. 10. Large-Strain Behavior: Effect of σ_y'/σ_0' on Undrained Shear Strength Normalized with Respect to Effective Confining Stress. Two Filled Circles Correspond to Destructured Specimens; Shaded Region Bounded by Dotted Lines Summarizes Data Published in Ladd and Foott (1974)

CONCLUSIONS

- The high void ratio and liquid limit of MC sediments point to a granular skeleton made of high-slenderness and high-specific-surface particles. The sensitivity of specific surface measurements to wet or dry test conditions confirms the presence of swelling minerals, detected in mineralogical studies.
- The small-strain stiffness is minimally sensitive to the state of stress below the yield stress $\sigma_0' < \sigma_y'$. The small-strain damping ratio between 6 and 10 Hz is controlled by viscous losses rather than frictional losses. When the yield stress exceeded $\sigma_0' > \sigma_y'$, the $G_{\max}$-stress exponent can be as high $\beta = 1.1$, which corresponds to a soil controlled by long-range electrical forces. The damping ratio reaches a peak near the yield stress, $\sigma_0' \approx \sigma_y'$.
- There is limited degradation in stiffness with the number of cycles at middle-strain level (cyclic). This is in agreement with the high plasticity and diagenetic overconsolidation of MC soils.
- The high effective-stress-strength parameters remain under study. The normalized undrained shear strength in triaxial compression is high, $(c_u/\sigma_0')_{NC} = 0.85$, in agreement with the high plasticity and specific surface of these soils. The normalized strength increases with the ratio between the yield stress and the effective confinement σ_y'/σ_0'; it decreases in destructured specimens and is lower in simple shear than in triaxial compression.
- Two strain thresholds are identified as separating the three strain regimes: the elastic threshold ($\gamma_{tl} = 3 \times 10^{-4}$) and the degradation threshold. Three alternatives are considered to determine the degradation threshold: pore pressure accumulation ($\gamma_{td} = 6$ to 8×10^{-3}); degradation in stiffness ($\gamma_{td} = 4$ to 8×10^{-3}); and cyclic degradation in strength ($\gamma_{td} = 3 \times 10^{-2}$). The strength criterion results in a higher degradation threshold, reflecting the decisive destructuring of the specimen required to attain strength loss.
- Bonds at interparticle contacts are preserved at strains below the elastic threshold. When strains exceed the degradation threshold, interparticle interaction between initially contiguous particles ceases. Additional mechanisms are expected at intermediate scales.

ACKNOWLEDGMENTS

This study has been supported by funds received from Dirección General de Apoyo al Personal Académico, Universidad Nacional Autonoma de México (UNAM), and from the Mid-America Earthquake Center under National Science Foundation Grant EEC-970185. The writers owe special thanks to F. Favela for providing support for this research. Reviewers provided detailed reviews and valuable suggestions. Y. H. Wang and E. Prencke (Georgia Tech) gathered the specific surface data. Editing of the manuscript was completed with the superb assistance of Guadalupe Salinas and Pedro Moreno.

REFERENCES

Barden, L. (1973). ''Theme 2, Macro and microstructure of soils.'' *Proc., Int. Symp. on Soil Struct.*, Swedish Geotechnical Society, Stockholm, 159–163.

Bennett, R. H., and Hulbert, M. H. (1986). *Clay microstructure*, International Human Resources Development Corporation, Boston.
Bjerrum, L. (1972). ''Embankments on soft ground.'' *Conf., Perf. of Earth and Earth-Supported Struct.*, ASCE, New York, Vol. 2, 1–54.
Bjerrum, L., and Simons, N. A. (1960). ''Comparison of shear strength characteristics of normally consolidated clays.'' *Proc., Res. Conf. on Shear Strength of Cohesive Soils*, ASCE, New York, 711–726.
Cascante, G., and Santamarina, J. C. (1996). ''Interparticle contact behavior and wave propagation.'' *J. Geotech. Engrg.*, ASCE, 122(10), 831–839.
Díaz-Rodríguez, J. A. (1989a). ''Behavior of Mexico City clay subjected to undrained repeated loading.'' *Can. Geotech. J.*, 26(1), 159–162.
Díaz-Rodríguez, J. A. (1989b). ''Effect of repeated loading on the strength of Mexico City clay.'' *4th Int. Conf. on Soil Dyn. and Earthquake Engrg.*, Computational Mechanics Publications, Southampton, Boston, 197–208.
Díaz-Rodríguez, J. A. (1992). ''On dynamic properties of Mexico City clay for wide strain range.'' *10th World Conf. on Earthquake Engrg.*, Vol. 1, Balkema, Rotterdam, The Netherlands, 1257–1262.
Díaz-Rodríguez, J. A., Lerouеil, S., and Alemán, J. D. (1992). ''Yielding of Mexico City clay and other natural clays.'' *J. Geotech. Engrg. Div.*, ASCE, 118(7), 981–995.
Díaz-Rodríguez, J. A., and López-Flores, L. (1999). ''A study of microstructure using resonant-column tests.'' *2nd Int. Conf. on Earthquake Geotech. Engrg.*, Vol. 1, Balkema, Rotterdam, The Netherlands, 89–94.
Díaz-Rodríguez, J. A., Lozano-Santa Cruz, R., Davila-Alcocer, V. M., Vallejo, E., and Girón, P. (1998). ''Physical, chemical, and mineralogical properties of Mexico City: A geotechnical perspective.'' *Can. Geotech. J.*, 35(4), 600–610.
Díaz-Rodríguez, J. A., Moreno, P., and Salinas, G. (2000). ''Undrained shear behavior of Mexico City sediments after cyclic loading.'' *12th World Conf. on Earthquake Engrg.*, Auckland, New Zealand (on CD-Rom).
Díaz-Rodríguez, J. A., and Santamarina, J. C. (1999). ''Thixotropy: The case of Mexico City soils.'' *11th Panamerican Conf. on Soil Mech. and Geotech. Engrg.*, Iguazu, Brazil. Vol. 1, 442–448.
Dobry, R. (1989). ''Some basic aspects of soil liquefaction during earthquakes: Earthquake hazards and design of constructed facilities in the Eastern United States.'' *Annals of New York Academy of Sci.*, 558, 172–182.
Dobry, R., and Vucetic, M. (1987). ''Dynamic properties and seismic response of soft clay deposits.'' *Proc., Int. Symp. on Geotech. Engrg. of Soft Soils*, Sociedad Mexicana de Mecanica de Suelos, Mexico City, Vol. 2, 49–85.
Fam, M., and Santamarina, J. C. (1997). ''A study of consolidation using mechanical and electromagnetic waves.'' *Géotechnique*, 47(2), 203–219.
Fam, M., Santamarina, J. C., and Dusseault, M. (1998). ''Wave-based monitoring processes in granular salt.'' *J. Envir. and Engrg. Geophys.*, 3(1), 15–26.
Farrar, D. M., and Coleman, J. D. (1967). ''The correlation of surface area with other properties of nineteen British clays.'' *J. Soil Sci.*, 18(1), 118–124.
Foreman, F. (1955). ''Palynology in southern North America. Part II: Study of two cores from lake sediments of the Mexico City Basin.'' *Geological Soc. of America Bull.*, 66, 475–510.
Ishihara, K. (1996). *Soil behaviour in earthquake geotechnics*, Clarendon Press, Oxford, U.K.
Kenney, T. C. (1959). ''Discussion to the paper 'Geotechnical properties of glacial clays.' by T. H. Wu.'' *J. Soil Mech. and Found. Div.*, ASCE, 85(3), 67–79.
Kokusho, T., Yoshida, Y., and Esashi, Y. (1982). ''Dynamic properties of soft clay for wide strain range.'' *Soils and Found.*, 22(4), 1–18.
Ladd, C. C., and Foott, R. (1974). ''New design procedure for stability of soft clays.'' *J. Geotech. Engrg. Div.*, ASCE, 100(7), 763–786.
Lo, K. Y. (1962). ''Shear strength properties of a sample of volcanic material of the Valley of Mexico.'' *Géotechnique*, 12(4), 303–318.
Marsal, R. J., and Mazari, M. (1959). ''*The subsoil of Mexico City*.'' Facultad de Ingeniería, Universidad Nacional Autónoma de México, Mexico City.
Marsal, R. J., and Salazar-Resines, J. (1960). ''Pore pressure and volumetric measurements in triaxial compression tests.'' *Proc., Res. Conf. on Shear Strength of Cohesive Soils*, ASCE, New York, 965–983.
Mesri, G., Rokhsar, A., and Bohor, B. F. (1975). ''Composition and compressibility of typical samples of Mexico City clay.'' *Géotechnique*, 25(3), 527–554.
Mitchell, J. K. (1993). *Fundamentals of soil behavior*, Wiley, New York.
Muhunthan, B. (1991). ''Liquid limit and surface area of clays.'' *Géotechnique*, 41(1), 135–138.
Ohara, S., and Matsuda, H. (1988). ''Study on the settlement of saturated clay layer induced by cyclic shear.'' *Soils and Found.*, 28(3), 103–113.
Peralta y Fabi, R. (1989). ''Sobre el origen de algunas propiedades mecánicas de la formación arcillosa superior del Valle de México.'' *Simposio sobre tópicos geológicos de la cuenca del Valle de México*, Sociedad Mexicana de Mecánica de Suelos, 43–53 (in Spanish).
Pusch, R. (1970). ''Microstructural changes in soft quick clay at failure.'' *Can. Geotech. J.*, 7, 1–7.
Santamarina, J. C., and Aloufi, M. (1999). ''Small strain stiffness: A Micromechanical experimental study.'' *Proc., Pre-failure Deformation Characteristics of Geomaterials*, M. Jamiolkowski, R. Lancellotta, and D. Lo Presti, eds., Torino, Italy, 451–458.
Santamarina, J. C., and Cascante, G. (1996). ''Stress anisotropy and wave propagation:a micromechanical view.'' *Can. Geotech. J.*, 33(5), 770–782.
Santamarina, J. C., Klein, K., and Fam, M. (2001). *Soils and waves*, Wiley, New York.
Terzaghi, K., Peck, R. B., and Mesri, G. (1996). *Soil mechanics in engineering practice*, Wiley, New York.
Vucetic, M. (1994). ''Cyclic threshold shear strains in soils.'' *J. Geotech. Engrg.*, ASCE, 120(12), 2208–2228.
Vucetic, M., and Dobry, R. (1991). ''Effect of soil plasticity on cyclic response.'' *J. Geotech. Engrg.*, ASCE, 117(1), 89–107.
Wood, D. (1990). *Soil behavior and critical state soil mechanics*, Cambridge University Press, New York.
Zeevaert, L. (1972). *Foundation engineering for difficult subsoil conditions*, Van Nostrand Reinhold, New York.
Zeevaert, L. (1991). ''Seismosoil dynamics of foundation in Mexico City earthquake, September 19, 1985.'' *J. Geotech. Engrg.*, ASCE, 117(3), 376–428.

NOTATION

The following symbols are used in this paper:

c_u = undrained strength;
D = average particle size;
d = interparticle distance;
e = void ratio;
e_{max} = maximum void ratio;
G_{max} = maximum shear modulus of soil;
g = gravity;
q_c = amplitude of cyclic load;
q_{cf} = residual quasistatic strength;
q_{sf} = initial monotonic strength;
R = ratio between amplitude of cyclic load and initial monotonic strength;
R_f = ratio between residual quasistatic strength and initial monotonic strength;
S_s = specific surface of particles;
S_u = undrained shear strength;
V_s = shear wave velocity;
α = slenderness of particles;
β = exponent;
γ = shear strain;
γ_{td} = degradation threshold strain;
γ_{tl} = linear threshold strain;
γ_{tv} = volumetric threshold strain;
γ_w = unit weight of water;
δ = relative displacement between contiguous soil particles;
ε = axial strain;
ζ = damping ratio of soil;
ρ_w = density of water;
ρ_m = density of mineral;
σ'_0 = isotropic confinement;
σ'_y = yielding stress;
σ'_{vo} = current vertical effective stress; and
ϕ' = internal friction angle of soil.